Thymic Selection Generates a Large T Cell Pool Recognizing a Self-Peptide in Humans

Alfred Zippelius,[1] Mikaël J. Pittet,[1] Pascal Batard,[1] Nathalie Rufer,[4] Magda de Smedt,[5] Philippe Guillaume,[6] Kim Ellefsen,[2] Danila Valmori,[1] Danielle Liénard,[1,3] Jean Plum,[5] H. Robson MacDonald,[6] Daniel E. Speiser,[1] Jean–Charles Cerottini,[6] and Pedro Romero[1]

[1]*Division of Clinical Onco-Immunology,* [2]*Division of Immunology and Allergy, and* [3]*Multidisciplinary Oncology Center, University Hospital (CHUV), 1011 Lausanne, Switzerland*
[4]*NCCR Molecular Oncology, Swiss Institute for Experimental Cancer Research, 1066 Epalinges, Switzerland*
[5]*Department of Clinical Chemistry, Microbiology and Immunology, University Hospital, 9000 Ghent, Belgium*
[6]*Ludwig Institute for Cancer Research, Lausanne Branch, University of Lausanne, 1066 Epalinges, Switzerland*

Abstract

The low frequency of self-peptide–specific T cells in the human preimmune repertoire has so far precluded their direct evaluation. Here, we report an unexpected high frequency of T cells specific for the self-antigen Melan-A/MART-1 in CD8 single–positive thymocytes from human histocompatibility leukocyte antigen-A2 healthy individuals, which is maintained in the peripheral blood of newborns and adults. Postthymic replicative history of Melan-A/MART-1–specific CD8 T cells was independently assessed by quantifying T cell receptor excision circles and telomere length ex vivo. We provide direct evidence that the large T cell pool specific for the self-antigen Melan-A/MART-1 is mostly generated by thymic output of a high number of precursors. This represents the only known naive self-peptide–specific T cell repertoire directly accessible in humans.

Key words: TREC • Telomere • Melan-A/MART-1 • naive • CD8

Introduction

The composition of self-peptide ligands present in the thymus plays a critical role in shaping the preimmune T cell repertoire (1, 2). Immature thymocytes expressing TCRs with low affinity for self-peptide/MHC survive and undergo further maturation (positive selection). Overtly autoreactive T cells are deleted by induction of programmed cell death (negative selection). Thereby, mature thymocytes with low affinity to self-peptide/MHC migrate to the periphery, founding a highly diverse T cell repertoire (3, 4). Additionally, self-peptide/MHC ligands deliver survival signals to naive T cells for their persistence in the periphery (5, 6). The recognition of self-peptides by T cells through the TCR has exquisite specificity as demonstrated by the drastic effects of single amino acid substitutions (7). However, the high degree of peptide cross-reactivity built in the T cell repertoire ensures recognition of virtually any presentable peptide. Synthetic peptide libraries contributed to the identification of multiple ligands that stimulate the same T cell clone without necessarily displaying sequence homology (8). It has been estimated that the frequency of individual epitope-specific naive T cells ranges around $1–5 \times 10^{-5}$ (9), which is below the limit of direct detection with currently available assays. TCR-transgenic approaches provide model systems for monitoring the selection process and in vivo fate of naive antigen–specific T cells (10). In humans, however, the low frequency of self-peptide–specific T cells in the preimmune repertoire has so far precluded their precise investigation.

A. Zippelius and M.J. Pittet contributed equally to this work.

Address correspondence to Pedro Romero, Division of Clinical Onco-Immunology, Ludwig Institute for Cancer Research, Hôpital Orthopédique, Niveau 5, Aile Est, Avenue Pierre Decker 4, 1005 Lausanne, Switzerland. Phone: 41-21-3140-176; Fax: 41-21-3147-477; E-mail: pedro.romero@isrec.unil.ch

The melanocyte differentiation antigen Melan-A/MART-1 (Melan-A)* is a self-protein of unknown function that is expressed by melanocytes and the majority of malignant melanoma cells, but not by other tissues (11, 12). HLA-A2–restricted Melan-A–specific CD8 T cells have been shown to primarily recognize the Melan-A 26–35 and 27–35 peptides (13, 14). Using HLA-A2 multimers synthesized around the Melan-A 26–35 A27L peptide analogue, we were able to identify Melan-A–specific T cells ex vivo in both tumor-infiltrated LNs and circulating lymphocytes of melanoma patients, as well as healthy individuals (15, 16). In the latter, Melan-A–specific T cells are phenotypically naive (CCR7+ CD45RA^{high} CD45RO− CD28+), and surprisingly comprise ∼10^{-3} of circulating CD8 T cells (17–19). This frequency is at least 10^2 times higher than the one currently estimated for naive antigen-specific lymphocyte precursors, and is comparable to that of epitope-specific memory CD8 T cells. This raises the question of how this unexpected large T cell pool is established and maintained. Obviously, the surface markers used in previous studies may not reliably reflect the functional state of Melan-A–specific T cells. In this regard, it has been shown that naive T cells may undergo expansion without phenotype change (20), or revert to a naive state after transient homeostasis-driven activation (21–23). Furthermore, memory T cells may revert to a naive phenotype (24). Alternatively, Melan-A–specific T cells may represent true naive lymphocytes due to increased life span in the periphery or increased thymic production.

In this study, we identified the mechanism for the existence of a large naive repertoire of T cells specific for the self-antigen Melan-A. Using MHC/peptide multimers, we enumerated Melan-A–specific T cells in the thymus and periphery of newborns and adults. To directly define the contribution of thymic production to this large self-specific T cell pool, we combined A2/Melan-A multimer labeling with measurement of postthymic replicative history by quantification of T cell receptor excision circles (TRECs) (25–27). During thymus development, formation of a productive TCR-α rearrangement requires deletion of the TCR-δ locus that is located within the TCR-α locus. Before TCR-α rearrangement, two TCR-δ–deleting elements, δRec and ψJα, preferentially rearrange to each other, thereby deleting the TCR-δ locus. The TCR-δ deletion product remains present as an extrachromosomal circle, the so-called signal joint TREC (28). TRECs are episomal excision circles that are stable, do not duplicate during mitosis, and consequently are diluted during cell division. We also measured the average length of telomere repeat sequences in Melan-A–specific T cells by quantitative fluorescence in situ hybridization and flow cytometry (flow FISH [29]), as an independent marker of their replicative history in vivo. Telomeres are specialized structures

at the end of eukaryotic chromosomes whose length decreases with age and population doublings in vitro. Despite transient telomerase activity, the telomere length of memory CD4 and CD8 T lymphocytes is significantly shorter than that of naive T cells (30, 31). For the first time, determination of TRECs and telomere length in antigen-specific CD8 T cells ex vivo provide direct evidence that a high frequency of thymic precursors is the predominant mechanism shaping the Melan-A–specific T cell preimmune repertoire. Implications for the presence of Melan-A cross-reactive ligands during thymic selection are discussed.

Materials and Methods

Tissues and Cells. Peripheral blood from 40 healthy donors (HD) that were 19–82-yr-old was collected at the Blood Transfusion Center (Lausanne, Switzerland). Three melanoma patients with stage III/IV disease who had undergone therapeutic tumor resection were selected for this study. After informed consent was obtained, tumor-infiltrated LNs (TILNs) were collected from patient LAU 465, and from patients LAU 359 and LAU 362. PBMCs from all patients were obtained at the time of surgery. Cord blood (CB) from 22 newborns and pediatric thymus tissue from 20 children who were 0–12-yr-old and had undergone corrective cardiac surgery, were collected at the University Hospital of Ghent (Ghent, Belgium), adhering to the guidelines of the Medical Ethical Commission of the hospital. Lymphocytes were prepared and cryopreserved as previously described (17). When indicated, lymphocytes were selected on the basis of HLA-A2 expression.

MHC/Peptide Multimers and mAbs. Synthesis of PE- and APC-labeled HLA-A2/peptide multimers was performed as previously described (15, 32). The peptides used were Melan-A$_{26–35}$ A27L (ELAGIGILTV), influenza matrix Flu-MA$_{58–66}$ (GILGFVFTL), CEA$_{694–702}$ (GVLVGVALI), gp100$_{209–218}$ T210M (IMDQVPFSV) (33), tyrosinase$_{368–376}$ (YMDGTMSQV), MAGE-4$_{254–262}$ (GVIDGRIHMV), MAGE-10$_{130–139}$, and NY-ESO-1$_{157–165}$ C165A (SLLMWITQA) (34). Because of the unstable binding of the Melan-A$_{26–35}$ natural peptide (EAAGIGILTV) to HLA-A2 (35), multimer synthesis around this peptide was performed using HLA-A2 molecules incorporating an unpaired cysteine residue at the COOH terminus, which allows site-specific biotinylation at 4°C (36). mAbs were from Becton Dickinson, except anti–CD45RO-FITC (Dako), anti–CD28-FITC (Immunotech), anti–perforin-FITC (Ancell), goat anti–rat IgG FITC (Southern Biotechnology Associates, Inc.), anti–CD8-ECD (Coulter Corp.), and goat anti–rat IgG APC (Caltag). Anti-CCR7 rat IgG mAb 3D12 and anti-2B4 rat IgG mAb were provided by Drs. M. Lipp and R. Forster (Max Delbrück Institute, Berlin, Germany), and Dr. M. Colonna (Basel Institute for Immunology, Basel, Switzerland), respectively.

FACS®. CD8 T lymphocytes were positively enriched from PBMCs and CB lymphocytes using CD8 microbeads (Miltenyi Biotec), whereas CD8 single positive (SP) thymocytes were negatively enriched using CD4 microbeads. Cells were stained with PE- and/or APC-labeled multimers for 1 h at room temperature in PBS, 0.2% BSA, 50 μM EDTA, and then incubated with appropriate mAbs for 20 min at 4°C. Cells were either immediately analyzed on a FACSCalibur® or sorted into defined populations on a FACSVantage® SE, using CellQuest software (Becton Dickinson). To maximize purification efficiency, the flow speed used during cell sorting corresponded to ∼2×10^3 cells per second. Purification of 5×10^3–2×10^5

---

*Abbreviations used in this paper: CB, cord blood; DP, double positive; flow FISH, fluorescence in situ hybridization and flow cytometry; HD, healthy donor; Melan-A, Melan-A/MART-1; SP, single positive; TILN, tumor infiltrated lymph node; TREC, T cell receptor excision circles.

A2/Melan-A$^+$ or A2/Flu-MA$^+$ cells required 5–12 h sorting. Immediate reanalysis of the isolated populations revealed >98% purification efficiency.

Quantitative PCR of TRECs. Quantification of signal joint (sj) TRECs in sorted CD8 T cells was performed by real time quantitative PCR with the 5′ nuclease (TaqMan) assay and an ABI7700 system (PerkinElmer). As previously described (25), cells were lysed in 100 mg/liter proteinase K (Roche Molecular Diagnostics) for 2 h at 56°C, and then for 15 min at 95°C. Each PCR reaction was performed in a 25-μl solution containing 5 μl of cell lysates, 12.5 μl of TaqMan® Universal Master Mix, including AmpliTaq Gold (Applied Biosystems), 500 nM of each primer (sj-5′ forward: CAC ATC CCT TTC AAC CAT GCT; sj-3′ reverse: GCC AGC TGC AGG GTT TAG G), and 125 nM probe (FAM-ACA CCT CTG GTT TTT GTA AAG GTG CCC ACT-TAMRA) in a final volume of 25 μl. The PCR conditions consisted of 1 cycle of 2 min at 50°C and 1 cycle of 10 min at 95°C, followed by 40 cycles of 30 s at 95°C and 1 min at 65°C. 10-fold serial dilutions ranging from 10^7 to 10^1 copies of sj internal standard provided by Dr. Daniel Douek (Vaccine Research Center, National Institute of Allergy and Infectious Diseases, Bethesda, MD), were tested in quadruplicates in each PCR experiment. A standard curve with a linear range across 7 logs DNA concentration was created, which calculated the number of TRECs in a given cell population. Thus, the lowest limit of quantification was considered to be 10 copies of the target sequence. In all PCR assays, the correlation coefficient of the standard curve was ≥0.997, whereas the slope varied between −3.52 and −3.67. TREC levels in total CD8 T cells and CCR7$^{+/-}$CD45RA$^{high/low}$ populations revealed comparable results when using 5×10^3–10^5 cells (linear regression analysis, $P < 0.001$; unpublished data). For each quantification, at least two independent cell sorting were performed and TREC levels were quantified by PCR in eight or more replicates.

Flow FISH. CD8 T cells were sorted ex vivo into 0.6–2 × 10^5 A2/Melan-A$^+$, A2/Flu-MA$^+$, naive CCR7$^+$CD45RA^{high}, and memory–effector non-CCR7$^+$CD45RA^{high} T cells. The average length of telomere repeats at chromosome ends in individual cells, was measured by quantitative flow FISH as previously described (29, 30). FITC-labeled fluorescent calibration beads (Quantum TM-24 Premixed; Bangs Laboratories Inc.) were used to convert telomere fluorescence data to molecules of equivalent soluble fluorescence (MESF) units. The following equation was performed to estimate the telomere length in basepair from telomere fluorescence in MESF units (bp = MESF × 0.495; [29]).

Cytolytic Activity. CD8 T cells were sorted ex vivo into 1–2 × 10^3 A2/Melan-A$^+$, A2/Flu-MA$^+$, and A2/multimer$^-$ cells on a FACSVantage® SE, and then stimulated with 1 μg/ml PHA-L, 150 U/ml IL-2, 10 ng/ml IL-7, and 10^6/ml allogeneic irradiated PBMCs. After 2 wk, the populations were >95% pure as assessed by multimer staining. Cells were tested for their lytic activity against peptide-pulsed HLA-A2$^+$ TAP-deficient T2 cells, and melanoma cells Na 8 (HLA-A2$^+$, Melan-A$^-$) or Me 290 (HLA-A2$^+$, Melan-A$^+$) in 4 h ^{51}Chromium release assays. The percentage of specific lysis was calculated as previously described (17).

Results

High Frequency of Circulating Melan-A–specific CD8 T Cells in Healthy HLA-A2 Individuals. We first determined the frequency of HLA-A2$^+$ adult individuals with a number of circulating Melan-A–specific CD8 T cells detectable by

staining with A2/Melan-A multimers. Staining of PBMCs from HLA-A2$^-$ individuals with these multimers has allowed the definition of a lower detection limit of 1 per 2,500 CD8 T cells (cut off = mean + 3 SD = 0.01% + 3 × 0.01% = 0.04%) under the experimental conditions used (17). Significant numbers of A2/Melan-A$^+$ cells were detected in 23 out of 31 (74%) HLA-A2$^+$ individuals (mean ± SD, 0.07% ± 0.04% of CD8 T cells). In contrast, CD8 T cells specific for other known self-peptides (CEA$_{694-702}$, gp100$_{208-218}$, tyrosinase$_{368-376}$, MAGE-4$_{130-139}$, MAGE-10$_{254-262}$, and NY-ESO-1$_{157-165}$) were not detectable. The data obtained in a positive individual (HD 009) are shown in Fig. 1 a. In this study, we used HLA-A2 multimers that were synthesized around the Melan-A
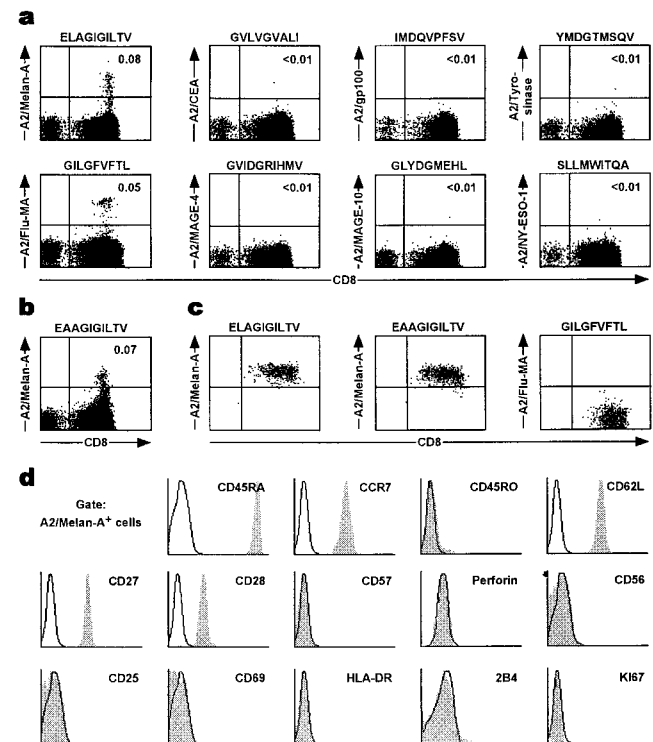

Figure 1. High frequency of phenotypically naive circulating Melan-A–specific CD8 T Cells in HLA-A2 healthy individuals. (a) Purified CD8 T cells from individual HD 009 were stained with anti-CD3, anti-CD8 mAbs, and HLA-A2 multimers synthesized around peptides derived from self-proteins (Melan-A$_{26-35}$ A27L analogue, CEA$_{694-702}$, gp-100$_{209-217}$ T210M analogue, tyrosinase$_{368-376}$, MAGE-4$_{130-139}$, MAGE-10$_{254-262}$, or NY-ESO-1$_{157-165}$ C165A analogue) and influenza matrix protein (Flu-MA$_{58-66}$). The sequence of each peptide is shown on the top of the corresponding dot plot. Figures in upper right quadrants are the percentages of multimer$^+$ cells in gated CD3$^+$CD8$^+$ cells. (b) Purified CD8 T cells from individual HD 009 were stained here with multimers synthesized around the Melan-A$_{26-35}$ natural peptide. (c) Purified Melan-A–specific CD8 T cells from individual HD 009, which had been expanded in vitro were stained with an anti-CD8 mAb, and multimers synthesized around the A27L Melan-A$_{26-35}$ A27L analogue (left), the Melan-A$_{26-35}$ natural peptide (middle), and the irrelevant influenza matrix$_{58-66}$ peptide (right). Dot plots are representative examples for six Melan-A–specific populations derived from PBMCs of adults and newborns, and from thymus. (d) Purified CD8 T cells from individual HD 009 were stained with A2/Melan-A multimers and a set of mAbs as indicated. Gated A2/Melan-A$^+$ cells are painted in gray and negative controls are in white.

A27L analogue peptide. The interchangeability between Melan-A A2/analogue (ELAGIGILTV) and A2/natural (EAAGIGILTV) peptide multimers has been previously demonstrated using tumor-specific CD8 T cells derived from melanoma patients (15). To confirm this finding in healthy individuals, we determined the frequency of circulating Melan-A–specific T cells from HD 009 that were detected with Melan-A A2/natural peptide multimers. As shown in Fig. 1 b, the frequency was similar to that obtained with Melan-A A2/analogue peptide multimers. Furthermore, we found that A2/Melan-A$^+$ populations, which had been expanded in vitro, were efficiently and specifically stained with multimers synthesized around either peptide (mean, 97%; SD, 6%, Fig. 1 c). Because of the unstable binding of the natural peptide to HLA-A2 (35), multimers synthesized around the A27L analogue peptide were used in further studies.

Previous reports have shown that circulating Melan-A–specific CD8 T cells from healthy individuals express the CD45RA, CCR7, and CD28 surface markers (17–19). In agreement with these results, we observed that A2/Melan-A$^+$ cells were homogeneously CD45RA^{high} CCR7$^+$ CD28$^+$ (mean, 95%; SD, 4%) in all individuals. Further analysis revealed that A2/Melan-A$^+$ cells were also CD27$^+$ CD45RO$^-$ CD56$^-$ CD57$^-$ CD62L$^+$ 2B4$^-$ perforin$^-$, and expressed neither the activation markers CD25, CD69, and HLA-DR, nor the proliferation marker Ki67 (Fig. 1 d). Altogether, these results indicate that a relatively high frequency of phenotypically naive Melan-A–specific T cells is detectable in the peripheral blood of the majority of healthy HLA-A2$^+$ individuals. In marked contrast, circulating A2/Flu-MA$^+$ cells, which we detected by multimer staining in 30 out of 31 (97%) HLA-A2$^+$ individuals (mean $\pm$ SD, 0.14% $\pm$ 0.16% of CD8 T cells; unpublished data), exhibit a memory CD45RA^{low} phenotype (84% $\pm$ 17%; unpublished data).

TREC Levels in CD8 T Cell Subsets. As a first approach to establish that circulating Melan-A–specific CD8 T cells are indeed naive, we determined TREC levels in naive versus memory/effector CD8 T cells. To this end, we sorted four subsets of circulating CD8 T cells on the basis of CCR7 and CD45RA expression (Fig. 2 a). This cell surface marker combination has recently been shown to effectively separate naive and memory/effector lym-

phocytes (37). TREC levels were measured in each CD8 T cell subset by quantitative PCR. In the four individuals tested, regardless of the age, TREC levels in the CCR7$^+$CD45RA^{high} subset were approximately one order of magnitude higher than in the three other subsets (Fig. 2 b). To validate these data, we estimated the average TREC levels in the whole CD8 T cell population by adding the TREC levels obtained for each T cell subset, and multiplying by their relative frequency (Fig. 2 b, reconstituted CD8$^+$). In all cases, these reconstituted values were comparable with the PCR-quantified TREC levels measured directly in the unfractionated autologous CD8 T cell population.

Melan-A–specific CD8 T Cells in Healthy Individuals Retain High TREC Levels and Long Telomeres. The results described above suggest that determination of TREC levels could provide useful information on the postthymic replicative history of circulating antigen-specific CD8 T cell populations. Therefore, we combined A2/peptide multimer-based cell separation and measurement of TRECs. Purified CD8 T cells from four HLA-A2 individuals were sorted into A2/Melan-A$^+$ (0.05–0.10% of CD8 T cells) and A2/Flu-MA$^+$ (0.05–0.21%) populations (Fig. 3 a). In parallel, naive (CCR7$^+$CD45RA^{high}) and memory/effector (non-CCR7$^+$CD45RA^{high}) CD8 T cell subsets were also sorted (Fig. 3 b). TREC levels were determined in each population, thus allowing a direct comparison between antigen-specific, naive, and memory/effector CD8 T cell populations derived from the same individual's blood sample. This analysis revealed relatively high levels of TRECs in A2/Melan-A$^+$ cells from all four individuals. TREC levels represented 47–69% (mean, 57%; SD, 9%) of those found in the autologous-naive CD8 T cells (Fig. 3 c), suggesting that on average, Melan-A–specific T cells have completed only one additional cell division. In marked contrast, TREC levels were below detection in purified A2/Flu-MA$^+$ cells (Fig. 3 c), and thus were similar to the levels observed in memory/effector CD8 T cells. It is thus apparent that on average, A2/Flu-MA$^+$ cells completed seven or more rounds of division as compared with autologous-naive and Melan-A–specific T cells.

As an independent approach, the average length of telomere repeats was measured in the four populations described above by flow FISH (29). Telomere length is
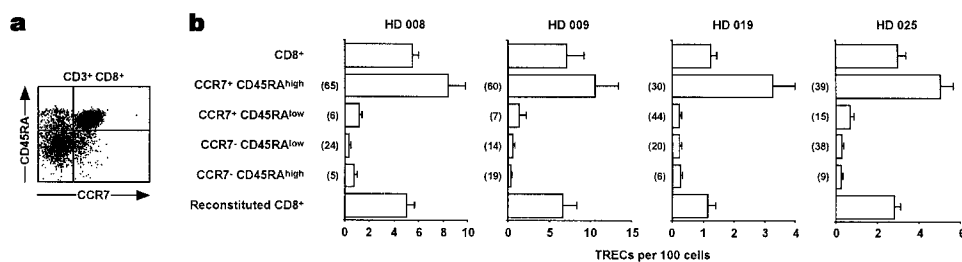

Figure 2. CCR7$^+$CD45RA^{high} CD8 T cells contain high levels of TRECs ex vivo. (a) Purified CD8 T cells were stained with anti-CD3, anti-CD8, anti-CCR7, and anti-CD45RA mAbs. Gated CD3$^+$CD8$^+$ cells were sorted into four subsets on the basis of CCR7 and CD45RA expression. (b) Real time PCR quantification of TRECs was performed in whole CD8 T cells (CD8$^+$) and in CCR7$^{+/-}$CD45RA$^{high/low}$ sorted subsets obtained from four individuals (HD 008, 009, 019, and 025). Figures in the left of each bar are the percentage of the corresponding subsets within whole CD8 T cells. TREC levels in whole CD8 T cells were also calculated by adding the TREC levels obtained for each CD8 T cell subset and multiplying by their relative frequency (reconstituted CD8$^+$).
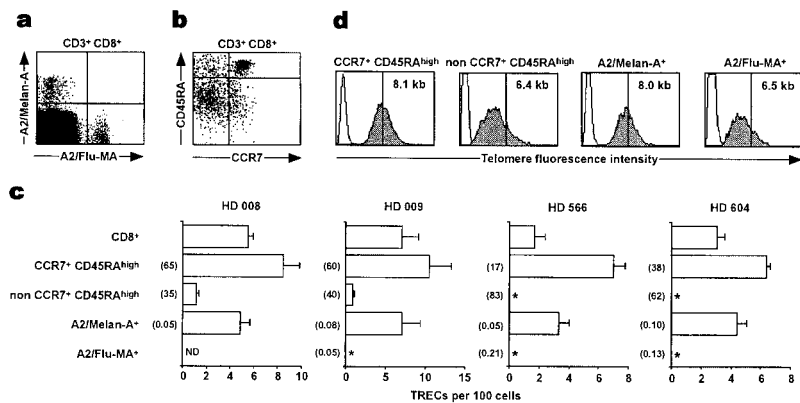
Figure 3. Melan-A–specific CD8 T cells in healthy individuals retain high TREC levels and long telomeres. (a) Purified CD8 T cells from HLA-A2 individuals were stained with anti-CD3 and anti-CD8 mAbs, together with PE-labeled A2/Melan-A and APC-labeled A2/Flu-MA multimers. Gated CD3⁺CD8⁺ cells were sorted into A2/Melan-A⁺ and A2/Flu-MA⁺ subsets. (b) Purified CD8 T cells were stained with anti-CD3, anti-CD8, anti-CCR7, and anti-CD45RA mAbs. Gated CD3⁺CD8⁺ cells were sorted into naive CCR7⁺CD45RA^high and memory/effector non-CCR7⁺CD45RA^high subsets. (c) Real time PCR quantification of TRECs was performed in whole CD8 T cells, in sorted naive and memory/effector subsets, and in sorted Melan-A and influenza-specific T cells (*, not detectable; ND, not done). Figures in the left of each bar are the percentage of the corresponding subsets in whole CD8 T cells. (d) Telomere fluorescence analysis was performed in sorted naive and memory/effector subsets, and Melan-A and influenza-specific CD8 T cells were obtained from individual HD 009. The telomere fluorescence was calculated by subtracting the mean background fluorescence from the mean fluorescence obtained with the telomere probe and is expressed in kilobase, as described in the Materials and Methods section.

an indicator of the replicative history of cells because lymphocytes gradually shorten their telomeres upon successive cell divisions (30). In agreement with the TREC data, both the naive and A2/Melan-A⁺ CD8 T cell populations displayed the brightest telomere fluorescence with a mean value corresponding to a telomere length of 8.1 and 8.0 kb, respectively. Measurement of the replicative history by assessing telomere length does not allow the detection of slight differences in the number of cell divisions between two populations. Thus, TREC dilution by ∼50% in the Melan-A–specific T cells compared with the autologous-naive CD8 T cells is not reflected by detectable changes in telomere length. In contrast, both the memory/effector and A2/Flu-MA⁺ CD8 T cell populations showed significantly reduced telomere fluorescence corresponding to a telomere loss of ∼1.6 kb (Fig. 3 d). The lack of TREC dilution and telomere shortening observed in Melan-A–specific CD8 T cells from healthy individuals provides direct evidence that they are naive.

Memory/Effector Melan-A–specific CD8 T Cells Display Reduced TREC Levels and Shortened Telomeres. We and other groups have demonstrated that in contrast to healthy individuals (Fig. 1 d), Melan-A specific–CD8 T cells may exhibit a memory/effector phenotype in patients with metastatic melanoma (15, 16, 18). To verify the relationship between phenotype shift and peripheral expansion in vivo, we determined the replicative history of Melan-A–specific T cells taken from three patients. In patient LAU 465 Melan-A–specific T cells were identified in PBMCs and TILNs (0.55% and 13% of CD8 T cells, respectively). From these cells, 84% and 100%, respectively, exhibited a memory/effector phenotype (Fig. 4 a). In contrast to our findings in healthy individuals, TRECs in A2/Melan-A⁺ PBMCs and TILNs were not detectable (Fig. 4 b). Identical observations were made with TILNs obtained from melanoma patients LAU 359 and LAU 362. Elevated frequencies of A2/Melan-A⁺ cells (2.1% and 0.7% of CD8 T cells, respectively) were identified by multimer staining. Again, the vast majority (>95%) of these cells exhibited a

memory/effector phenotype and did not contain detectable levels of TRECs (unpublished data). In line with these observations, the mean relative telomere length of sorted A2/Melan-A⁺ TILNs from patient LAU 465 was comparable to that measured in circulating memory/effector autologous CD8 T cells (Fig. 4 d, corresponding to 6.9-kb telomere length). This represents a telomere shortening of 2.4 kb with respect to autologous naive CD8 T cells, indicating extensive proliferation in vivo.

High Frequency of Melan-A–specific CD8 T Cells in Newborns. We next investigated whether the high frequency of circulating Melan-A–specific CD8 T cells is already detectable in newborns. For this purpose, we stained HLA-
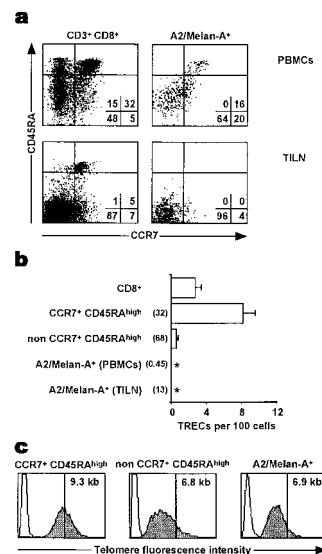

Figure 4. Memory/effector Melan-A–specific CD8 T cells display reduced TREC levels and shortened telomeres. (a) Purified CD8 T cells were obtained from PBMCs (top) and TILNs (bottom) of melanoma patient LAU 465. In the left panels, lymphocytes were stained with anti-CD3, anti-CD8, anti-CCR7, and anti-CD45RA mAbs, and dot plots are shown for gated CD3⁺CD8⁺ cells. In the right panels, lymphocytes were stained with anti-CCR7, anti-CD45RA mAbs, and A2/Melan-A multimers, and dot plots are shown for gated A2/Melan-A⁺ cells. (b) Real time PCR quantification of TRECs was performed in whole CD8 T cells, in sorted naive and memory/effector CD8 T cells from PBMCs, and in sorted Melan-A–specific T cells from both PBMCs and TILNs (*, not detectable). Figures in the left of each bar are the percentage of the corresponding subsets in CD8 T cells. (c) Telomere fluorescence analysis was performed in sorted naive and memory/effector CD8 T cells from PBMCs, and Melan-A–specific CD8 T cells from TILNs. Telomere fluorescence was calculated as in Fig. 3 d, and is expressed in kilobase (see Materials and Methods).

A2[+] CB lymphocytes with A2/Melan-A multimers. The lower limit of detection was 0.04% of CD8 T cells, as determined by A2/Melan-A multimer staining on 11 HLA-A2[−] CB lymphocyte samples (cut off = mean + 3 SD = 0.01% + 3 × 0.01%; unpublished data). Significant numbers of A2/Melan-A^{+} cells in CB were detected in 9 out of 11 (82%) HLA-A2[+] newborns (Fig. 5 a, mean ± SD, 0.10% ± 0.04% of CD8 T cells). In contrast, A2/Flu-MA^{+} cells were not detected in CB (Fig. 5 b, <0.01%). A2/Melan-A^{+} CB cells were CD45RA^{high} (mean ± SD, 94% ± 4%) and CCR7^{+} (96% ± 4%) in 7 out of 7 individuals (Fig. 5 c, shown representatively as CB 15). In line with a naive phenotype, A2/Melan-A^{+} cells from CB 15 contained high levels of TRECs (Fig. 5 d). As compared with the autologous CD8 T cell pool, Melan-A–specific T cells contained 74% of TRECs, indicating that on average they had completed less than one cell division. Thus, the postthymic replicative history of Melan-A–specific T cells is similar in newborns and adults, consistent with the possibility that these cells represent recent thymic emigrants.

High Frequency of Melan-A–specific CD8 SP Thymocytes. To directly investigate the origin of the Melan-A–specific CD8 T cell repertoire, we performed multimer staining of lymphocytes derived from human thymus. Double positive (DP) thymocytes form the vast majority of cells found in the thymus. They express low levels of α/β TCR and are programmed to die within 3 to 4 d unless rescued by a TCR signal. 1–5% of the DP cells survive, increase TCR expression, and mature to CD4 and CD8 SP cells. Cell surface expression of TCR may allow direct identification of antigen-specific cells in both the DP and SP stages of T cell development by staining with A2/peptide multimers. However, neither A2/Melan-A[+] nor A2/Flu-MA^{+} cells were detected in the pool of DP thymocytes (<0.01%; unpublished data). We further investigated the presence of

antigen-specific cells in the pool of CD8 SP thymocytes. Staining of CD4-depleted thymocytes from nine HLA-A2[−] individuals with A2/Melan-A multimers revealed a lower limit of detection of 0.04% of CD8 SP cells (cut off = mean + 3 SD = 0.01% + 3 × 0.01%, unpublished data). Similar analysis with HLA-A2[+] thymocytes revealed that significant numbers of A2/Melan-A[+] CD8 SP cells were detectable in six out of nine (67%) individuals (Fig. 5 e, mean ± SD, 0.04% ± 0.01% of CD8 T cells). As expected, A2/Melan-A^{+} cells were not detectable in CD4 SP cells (<0.01%; unpublished data). Furthermore, A2/Flu-MA^{+} cells were not detected in the thymus (<0.01% of DP, CD4 SP, and CD8 SP cells; Fig. 5 f, and unpublished data). Altogether, our results indicate that a high frequency of Melan-A–, but not influenza-specific CD8 SP precursors are generated in the human thymus.

Functional Potential of Melan-A–specific CD8 SP Thymocytes. We assessed the functional potential of Melan-A–specific CD8 T cells sorted from thymocytes of patient 02. After mitogen-driven expansion in vitro, the A2/Melan-A^{+} population exhibited an activated phenotype (CCR7^{−} CD45RA^{low} CD45RO^{+} CD27^{int} CD28^{−} CD62L^{−} CD69^{int} HLA-DR^{+}, unpublished data). As presented in Fig. 6 a, thymus-derived A2/Melan-A^{+} cells specifically lysed T2 cells in the presence of the Melan-A$_{26–35}$ natural (EAAGIGILTV) or the analogue (ELAGIGILTV) peptide, whereas no lysis was noticed in the presence of the irrelevant influenza matrix$_{58–66}$ (GILGFVFTL) peptide. Furthermore, peptide titration curves confirmed the fine specificity of Melan-A peptide recognition observed in previous studies (15, 35). Thymus-derived A2/Melan-A^{+} cells also exhibited a high lytic activity against the HLA-A2[+] Melan-A[+] Me 290 tumor cell line, but not against the HLA-A2[+] Melan-A[−] Na 8 tumor cell line (Fig. 6 b). Comparable results were obtained with Melan-A–specific
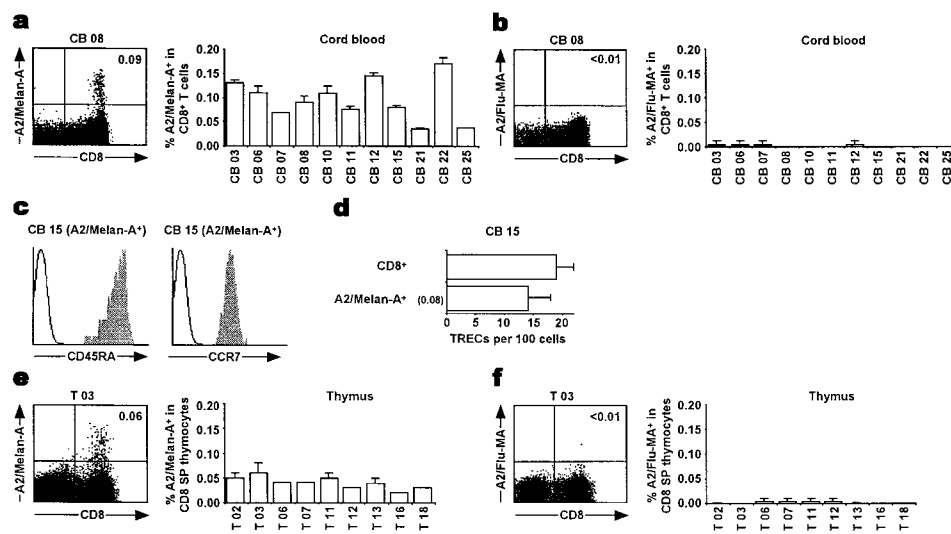

Figure 5. High frequency of Melan-A–specific CD8 T cells in CB and thymus. (a and b) Purified CD8 T cells from 11 CB specimens were stained with anti-CD3, anti-CD8 mAbs, and A2/Melan-A (a), or A2/Flu-MA (b) multimers. The percentage of A2/peptide multimer^{+} cells is given in gated CD3^{+}CD8^{+} lymphocytes. (c) Purified CB CD8 T cells were stained with A2/Melan-A multimers, anti-CD3, anti-CD8, and anti-CD45RA (left) or anti-CCR7 (right) mAbs. Histograms are shown for gated CD3^{+}CD8^{+}A2/Melan-A^{+} cells and are representative examples for seven individuals. Gated A2/Melan-A^{+} cells are painted in gray and negative controls are in white. (d) Real time PCR quantification of TRECs was performed in whole CB CD8 T cells and in Melan-A–specific T cells (0.08% of CD8 T cells) from CB15. TREC levels in CD8 T cells are representative for four individuals. (e and f) CD4-depleted thymocytes from nine thymus specimens were stained with anti-CD3, anti-CD4, anti-CD8 mAbs, and A2/Melan-A (e) or A2/Flu-MA (f) multimers. The percentage of A2/peptide multimer^{+} cells is given in CD3^{high}CD4^{−}CD8^{+} thymocytes.
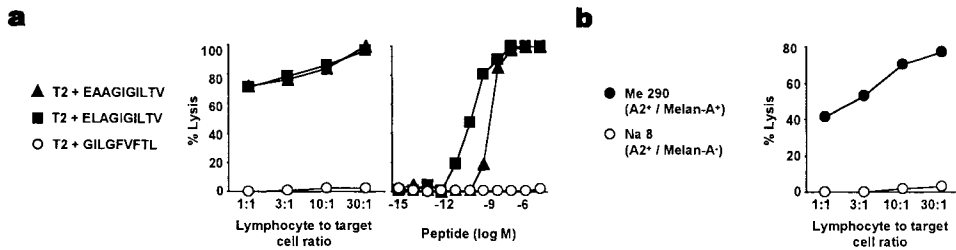
Figure 6. Functional potential of Melan-A–specific CD8 SP thymocytes. (a) Purified Melan-A–specific CD8 SP thymocytes, which had been expanded in vitro, were tested in a 4-h ^{51}Cr-release assay for their cytolytic activity against A2$^+$ TAP-deficient T2 cells in the presence of exogenously added Melan-A$_{26-35}$ (▲), Melan-A$_{26-35}$ A27L analogue (■), or irrelevant influenza matrix$_{58-66}$ peptides (○). In lymphocyte to target cell ratio titrations (left), peptides were used at 1 μM. In peptide titrations (right), the lymphocyte to target cell ratio used was 10:1. Results are representative examples for six Melan-A–specific T cell populations derived from thymus and peripheral blood of newborns and adults. (b) Purified Melan-A–specific CD8 SP thymocytes, which had been expanded in vitro, were tested in a 4-h ^{51}Cr-release assay for their cytolytic activity against Me 290 (●, A2$^+$ / Melan-A$^+$) and Na 8 (○, A2$^+$ / Melan-A$^-$) tumor cells. Results are representative examples for six Melan-A–specific T cell populations derived from thymus and peripheral blood of newborns and adults.

T cells sorted from CB of newborns 07 and 08, and of adults HD 008, HD 009, and HD 604 (unpublished data). Thus, Melan-A–specific T cells already present in a high frequency in the thymus have the capacity to efficiently recognize endogenously produced Melan-A peptide(s).

Discussion

Although abundantly present in the mature T cell repertoire of HLA-A2 adult individuals, circulating Melan-A–specific CD8 T cells display a naive phenotype (17–19). In this study, we directly identified the origin of the large Melan-A–specific T cell pool. First, high numbers of Melan-A–specific T cells are already detected in CD8 SP thymocytes and are maintained in the mature T cell repertoire of newborns and adults. Second, high TREC levels and long telomeres are retained in circulating Melan-A–specific T cells and are comparable with those found in autologous-naive lymphocytes. Together, these results demonstrate that the shaping of the preimmune T cell repertoire specific for the self-antigen Melan-A is mostly imposed by thymic output of a high frequency of precursors. Thus, the size of the circulating Melan-A–specific T cell pool in adults is at least 10^2 times larger than current estimates for naive antigen-specific lymphocyte precursors, and approaches that of epitope-specific memory CD8 T cells.

Melan-A–specific thymocytes cannot be found in DP cells, but become detectable in CD8 SP cells. The selective detection of Melan-A–specific T cells in the latter subset may be explained by at least two reasons. First, the lower levels of TCR α/β molecules on DP thymocytes may not be sufficient for efficient staining with MHC/peptide multimers. Second, the frequency of Melan-A–specific thymocytes is probably highly diluted in the DP stage by the >95% cells that will not reach the SP pool. Nonetheless, our findings clearly show that a high frequency of Melan-A–specific precursors is selected in the human thymus. Once they have completed their thymic maturation, these cells are seeded and maintained at high numbers in the peripheral blood ($\sim10^{-3}$ of circulating CD8 T cells), representing a total number of 0.5–2 × 10^6 cells. Because 98% of all lymphocytes are sequestered in tissues (38), it is possible that $25-100 × 10^6$ cells recognizing the self-antigen

Melan-A persist in the peripheral lymphoid compartment. In marked contrast, influenza-specific T cells are below detection both in the thymus and in newborns, and only become detectable in adult individuals, most likely driven by extensive clonal expansion in response to viral infection.

The simplest explanation for the high frequency of circulating Melan-A–specific CD8 T cells is peripheral expansion. This possibility, however, is ruled out by parameters reflecting the replicative history of circulating Melan-A–specific T cells (TREC levels and telomere length). The TREC levels in a naive T cell population at any time will be determined by factors inclusive of thymic production and T cell homeostasis (assuming no intracellular TREC decay). As peripheral T cell division substantially affects the intracellular TREC content (27), the availability of TREC levels from thymocytes to mature peripheral lymphocytes allows the calculation of the post-thymic replicative history of CD8 T cells. If we first consider CB, we may estimate that on average, CD8 T cells in newborns (mean ± SD, 24 ± 5 TRECs in 100 cells) completed one to two population doublings relative to CD8 SP thymocytes (57 ± 7 TRECs per 100 cells; unpublished data). Such limited cell division may be controlled by continued specific recognition of self-peptide/MHC, responsible for the persistence of mature lymphocytes in the periphery (5, 6). In peripheral blood of adults, CD8 T cells include two groups with distinct replicative histories. Naive (CCR7$^+$CD45RA^{high}) CD8 T cells (7 ± 3 TRECs per 100 cells) completed approximately three population doublings, whereas on average, memory/effector (non-CCR7$^+$CD45RA^{high}) CD8 T cells (0.5 ± 0.4 TRECs per 100 cells) underwent seven population doublings in the periphery. The strikingly different replicative histories of CCR7$^+$CD45RA^{high} and non-CCR7$^+$CD45RA^{high} subsets confirm that the combination of CCR7 and CD45RA surface markers allows the distinction of naive from memory/effector lymphocytes. This conclusion is further supported by the finding that naive lymphocytes exhibit significantly longer telomeres as compared with their memory/effector counterparts. Furthermore, the relative telomere length of naive lymphocytes is quite uniform, indicating that these cells represent a homogeneous population. If we now consider antigen-specific CD8 T cells,

Melan-A–specific T cells in CB (mean ± SD, 14 ± 4 TRECs per 100 cells) reveal a proliferative history compared with that of the whole CD8 T cell pool. Likewise, Melan-A–specific T cells in peripheral blood of adults (5 ± 2 TRECs per 100 cells) resemble the naive CD8 T cell pool, as they also completed limited cell division. Indeed, the data suggest that on average, Melan-A specific T cells have only completed one cell division compared with the autologous-naive subset (TREC dilution by ~50%). This may reflect a slightly increased division rate and/or prolonged life span. In either case, the net effect would be the observed consistently lower TREC content as compared with the autologous naive CD8 T cells. Because all Melan-A–specific T cells homogeneously retain long telomeres ex vivo, it also implies that most cells in the pool underwent a similar number of divisions. In marked contrast to Melan-A–specific T cells, influenza-specific T cells have an extensive replicative history in the periphery of adults. Because their TRECs are not detectable, the virus-specific T cells completed >10 population doublings. In this case a single thymocyte precursor may generate >10^3 CD8 T cell progeny. This is in line with the recent finding that after antigenic stimulation, naive CD8 T cells become committed to dividing at least seven times and differentiating into memory/effector cells (39). In agreement with these data, we observed significant telomere shortening of influenza-specific T cells as compared with autologous-naive CD8 T cells.

Accumulating evidence indicates a central role for self-peptides in thymic selection. Interestingly, previous experiments showed that Melan-A mRNA is not detectable in the thymus, which suggests that the large Melan-A–specific T cell pool might be shaped in the absence of the selecting and/or deleting ligand (12). In this respect, it is noteworthy that the Melan-A peptide sequence, recognized by CD8 T cells from HLA-A2 individuals, is localized in the putative hydrophobic transmembrane domain of the protein, which greatly limits the diversity of its amino acid composition. Indeed, sequence homology between the Melan-A peptide and a broad range of self-derived proteins has recently been reported (40, 41). Consequently, recognition of Melan-A–cross-reactive ligands may play an important role in positive thymic selection by generating a large naive T cell pool. Based on previous experimental work (42), we hypothesize that highly specific interactions between self-peptides and TCR, rather than promiscuous recognition, are driving the positive selection process. However, since there is increasing evidence that a wide variety of tissue-specific antigens may be weakly expressed intrathymically (43), we cannot exclude the possibility that weak expression of Melan-A in the thymus may also result in the deletion of high-avidity CD8 T cells (3, 4, 10). It will be important to determine which sequence motifs are involved in positive thymic selection of Melan-A–specific T cells. Preliminary experiments seem to indicate that generation of the large Melan-A–specific T cell pool is not due to selection of a particular TCR. Indeed, we investigated the TCR-β repertoire of Melan-A–specific CD8 T cells ex vivo in HD 009 by using multimers in conjunction with anti-CD8 and anti–TCR-β chain variable (BV) mAbs. This analysis revealed that at least 13 out of 18 BV segments investigated were used (BV1, 2, 3, 7, 8, 13.1, 13.6, 14, 16, 17, 20, 21, 22), each representing 2–10% of the whole Melan-A–specific repertoire (unpublished data). It is noteworthy that analysis of complementary determining region-3 length, and sequence of activated Melan-A–specific cells in tumor-infiltrated lymph nodes from melanoma patients, indicated that these cells display a large and highly diverse TCR-β repertoire (44).

The mechanisms preventing the activation of circulating Melan-A–specific CD8 T cells are unknown. It is conceivable that the lack of peripheral activation reflects ignorance (45, 46). Indeed, expression of Melan-A is restricted to cells of the melanocytic lineage, including subepidermal melanocytes, retinal pigmented epithelial cells, and choroidal melanocytes, which are physiologically concealed from the immune system. In addition, skin melanocytes are only ~5% of the total skin cell pool, and thus there is a relatively low abundance of the Melan-A antigen. Both spatial segregation and low levels of Melan-A might explain why the circulating Melan-A–specific T cell pool is virtually never activated, despite frequent skin injury during the lifetime of adults, and thus remains ignorant. In marked contrast, Melan-A–specific T cells can be activated in patients with malignant melanoma or rare autoimmune disorders. The vast majority of melanoma patients contains detectable accumulations of memory/effector Melan-A–specific T cells in metastatic tumor lesions (Fig. 4 [15, 47]). Thus, in the appropriate milieu, including a high antigen load and disruption of tissue architecture brought about by tumor progression, Melan-A–specific T cells successfully overcome ignorance and undergo clonal expansion. As documented here, the emergence of memory/effector lymphocytes in the Melan-A– specific T cell pool of melanoma patients is accompanied by TREC dilution and telomere shortening. It has also been suggested that Melan-A–specific T cells may destroy melanocytes in the eyes of patients with Vogt-Koyanagi-Harada disease and sympathetic ophthalmia, which are systemic inflammatory disorders that affect tissues containing melanocytes (48). Finally, the observation of an elevated frequency of Melan-A–specific T cells in vitiligo patients also underlines the involvement of these cells in autoimmune destruction of skin melanocytes (49, 50).

The key finding in this study is that a large pool of human-naive CD8 T lymphocytes specific for the self-antigen Melan-A can be identified and characterized by multimer staining in the thymus and peripheral lymphoid compartment of healthy individuals. Our results provide direct evidence that this T cell pool is generated by thymic output of a high frequency of precursors that undergo limited cell division in the periphery. It will be of great interest to identify the ligands involved in selecting and maintaining such an abundant self-specific naive T cell repertoire.

References

1. Goldrath, A.W., and M.J. Bevan. 1999. Selecting and maintaining a diverse T-cell repertoire. *Nature.* 402:255–262.

2. Sprent, J., and H. Kishimoto. 2001. The thymus and central tolerance. *Philos. Trans. R. Soc. Lond. B Biol. Sci.* 356:609–616.

3. Sandberg, J.K., L. Franksson, J. Sundback, J. Michaelsson, M. Petersson, A. Achour, R.P. Wallin, N.E. Sherman, T. Bergman, H. Jornvall, et al. 2000. T cell tolerance based on avidity thresholds rather than complete deletion allows maintenance of maximal repertoire diversity. *J. Immunol.* 165:25–33.

4. de Visser, K.E., T.A. Cordaro, D. Kioussis, J.B. Haanen, T.N. Schumacher, and A.M. Kruisbeek. 2000. Tracing and characterization of the low-avidity self-specific T cell repertoire. *Eur. J. Immunol.* 30:1458–1468.

5. Ernst, B., D.S. Lee, J.M. Chang, J. Sprent, and C.D. Surh. 1999. The peptide ligands mediating positive selection in the thymus control T cell survival and homeostatic proliferation in the periphery. *Immunity.* 11:173–181.

6. Viret, C., F.S. Wong, and C.A. Janeway, Jr. 1999. Designing and maintaining the mature TCR repertoire: the continuum of self-peptide:self-MHC complex recognition. *Immunity.* 10:559–568.

7. Hemmer, B., C. Pinilla, B. Gran, M. Vergelli, N. Ling, P. Conlon, H.F. McFarland, R. Houghten, and R. Martin. 2000. Contribution of individual amino acids within MHC molecule or antigenic peptide to TCR ligand potency. *J. Immunol.* 164:861–871.

8. Pinilla, C., V. Rubio-Godoy, V. Dutoit, P. Guillaume, R. Simon, Y. Zhao, R.A. Houghten, J.C. Cerottini, P. Romero, and D. Valmori. 2001. Combinatorial peptide libraries as an alternative approach to the identification of ligands for tumor-reactive cytolytic T lymphocytes. *Cancer Res.* 61:5153–5160.

9. Mason, D. 1998. A very high level of crossreactivity is an essential feature of the T-cell receptor. *Immunol. Today.* 19:395–404.

10. Bouneaud, C., P. Kourilsky, and P. Bousso. 2000. Impact of negative selection on the T cell repertoire reactive to a self-peptide: a large fraction of T cell clones escapes clonal deletion. *Immunity.* 13:829–840.

11. Coulie, P.G., V. Brichard, A. Van Pel, T. Wolfel, J. Schneider, C. Traversari, S. Mattei, E. De Plaen, C. Lurquin, and J.P. Szikora. 1994. A new gene coding for a differentiation antigen recognized by autologous cytolytic T lympho-

12. Kawakami, Y., S. Eliyahu, C.H. Delgado, P.F. Robbins, L. Rivoltini, S.L. Topalian, T. Miki, and S.A. Rosenberg. 1994. Cloning of the gene coding for a shared human melanoma antigen recognized by autologous T cells infiltrating into tumor. *Proc. Natl. Acad. Sci. USA.* 91:3515–3519.

13. Kawakami, Y., S. Eliyahu, K. Sakaguchi, P.F. Robbins, L. Rivoltini, J.R. Yannelli, E. Appella, and S.A. Rosenberg. 1994. Identification of the immunodominant peptides of the MART-1 human melanoma antigen recognized by the majority of HLA-A2–restricted tumor infiltrating lymphocytes. *J. Exp. Med.* 180:347–352.

14. Romero, P., N. Gervois, J. Schneider, P. Escobar, D. Valmori, C. Pannetier, A. Steinle, T. Wolfel, D. Lienard, V. Brichard, et al. 1997. Cytolytic T lymphocyte recognition of the immunodominant HLA-A*0201-restricted Melan-A/MART-1 antigenic peptide in melanoma. *J. Immunol.* 159:2366–2374.

15. Romero, P., P.R. Dunbar, D. Valmori, M. Pittet, G.S. Ogg, D. Rimoldi, J.L. Chen, D. Lienard, J.C. Cerottini, and V. Cerundolo. 1998. Ex vivo staining of metastatic lymph nodes by class I major histocompatibility complex tetramers reveals high numbers of antigen-experienced tumor-specific cytolytic T lymphocytes. *J. Exp. Med.* 188:1641–1650.

16. Pittet, M.J., D.E. Speiser, D. Lienard, D. Valmori, P. Guillaume, V. Dutoit, D. Rimoldi, F. Lejeune, J.C. Cerottini, and P. Romero. 2001. Expansion and functional maturation of human tumor antigen–specific CD8+ T cells after vaccination with antigenic peptide. *Clin. Cancer Res.* 7:796s–803s.

17. Pittet, M.J., D. Valmori, P.R. Dunbar, D.E. Speiser, D. Lienard, F. Lejeune, K. Fleischhauer, V. Cerundolo, J.C. Cerottini, and P. Romero. 1999. High frequencies of naive Melan-A/MART-1–specific CD8+ T cells in a large proportion of human histocompatibility leukocyte antigen (HLA)-A2 individuals. *J. Exp. Med.* 190:705–715.

18. Dunbar, P.R., C.L. Smith, D. Chao, M. Salio, D. Shepherd, F. Mirza, M. Lipp, A. Lanzavecchia, F. Sallusto, A. Evans, et al. 2000. A shift in the phenotype of melan-A-specific CTL identifies melanoma patients with an active tumor-specific immune response. *J. Immunol.* 165:6644–6652.

19. Pittet, M.J., A. Zippelius, D.E. Speiser, M. Assenmacher, P. Guillaume, D. Valmori, D. Lienard, F. Lejeune, J.C. Cerottini, and P. Romero. 2001. Ex vivo IFN-gamma secretion by circulating CD8 T lymphocytes: implications of a novel approach for T cell monitoring in infectious and malignant diseases. *J. Immunol.* 166:7634–7640.

20. Unutmaz, D., P. Pileri, and S. Abrignani. 1994. Antigen-independent activation of naive and memory resting T cells by a cytokine combination. *J. Exp. Med.* 180:1159–1164.

21. Goldrath, A.W., L.Y. Bogatzki, and M.J. Bevan. 2000. Naive T cells transiently acquire a memory-like phenotype during homeostasis-driven proliferation. *J. Exp. Med.* 192:557–564.

22. Cho, B.K., V.P. Rao, Q. Ge, H.N. Eisen, and J. Chen. 2000. Homeostasis-stimulated proliferation drives naive T cells to differentiate directly into memory T cells. *J. Exp. Med.* 192:549–556.

23. Murali-Krishna, K., and R. Ahmed. 2000. Cutting edge: naive T cells masquerading as memory cells. *J. Immunol.* 165:1733–1737.

24. Hargreaves, M., and E.B. Bell. 1997. Identical expression of CD45R isoforms by CD45RC+ 'revertant' memory and CD45RC+ naive CD4 T cells. *Immunology.* 91:323–330.

25. Douek, D.C., R.D. McFarland, P.H. Keiser, E.A. Gage, J.M.

Massey, B.F. Haynes, M.A. Polis, A.T. Haase, M.B. Feinberg, J.L. Sullivan, et al. 1998. Changes in thymic function with age and during the treatment of HIV infection. *Nature.* 396:690–695.

26. Poulin, J.F., M.N. Viswanathan, J.M. Harris, K.V. Komanduri, E. Wieder, N. Ringuette, M. Jenkins, J.M. McCune, and R.P. Sekaly. 1999. Direct evidence for thymic function in adult humans. *J. Exp. Med.* 190:479–486.

27. Hazenberg, M.D., S.A. Otto, J.W. Cohen Stuart, M.C. Verschuren, J.C. Borleffs, C.A. Boucher, R.A. Coutinho, J.M. Lange, T.F. Rinke de Wit, A. Tsegaye, et al. 2000. Increased cell division but not thymic dysfunction rapidly affects the T-cell receptor excision circle content of the naive T cell population in HIV-1 infection. *Nat. Med.* 6:1036–1042.

28. Verschuren, M.C., I.L. Wolvers-Tettero, T.M. Breit, J. Noordzij, E.R. van Wering, and J.J. van Dongen. 1997. Preferential rearrangements of the T cell receptor-delta-deleting elements in human T cells. *J. Immunol.* 158:1208–1216.

29. Rufer, N., W. Dragowska, G. Thornbury, E. Roosnek, and P.M. Lansdorp. 1998. Telomere length dynamics in human lymphocyte subpopulations measured by flow cytometry. *Nat. Biotechnol.* 16:743–747.

30. Rufer, N., T.H. Brummendorf, S. Kolvraa, C. Bischoff, K. Christensen, L. Wadsworth, M. Schulzer, and P.M. Lansdorp. 1999. Telomere fluorescence measurements in granulocytes and T lymphocyte subsets point to a high turnover of hematopoietic stem cells and memory T cells in early childhood. *J. Exp. Med.* 190:157–167.

31. Weng, N.P., B.L. Levine, C.H. June, and R.J. Hodes. 1995. Human naïve and memory T lymphocytes differ in telomeric length and replicative potential. *Proc. Natl. Acad. Sci. USA.* 92:11091–11094.

32. Altman, J.D., P.A.H. Moss, P.J.R. Goulder, D.H. Barouch, M.G. McHeyzer-Williams, J.I. Bell, A.J. McMichael, and M.M. Davis. 1996. Phenotypic analysis of antigen-specific T lymphocytes. *Science.* 274:94–96 (erratum published 280:1821).

33. Rosenberg, S.A., J.C. Yang, D.J. Schwartzentruber, P. Hwu, F.M. Marincola, S.L. Topalian, N.P. Restifo, M.E. Dudley, S.L. Schwarz, P.J. Spiess, et al. 1998. Immunologic and therapeutic evaluation of a synthetic peptide vaccine for the treatment of patients with metastatic melanoma. *Nat. Med.* 4:321–327.

34. Romero, P., V. Dutoit, V. Rubio-Godoy, D. Liénard, P. Guillaume, C. Servis, D. Rimoldi, J.C. Cerottini, and D. Valmori. 2001. CD8+ T cell response to NY-ESO-1: relative antigenicity and in vitro immunogenicity of natural and analogue sequences. *Clin. Cancer Res.* 7:766s–772s.

35. Valmori, D., J.F. Fonteneau, C.M. Lizana, N. Gervois, D. Lienard, D. Rimoldi, V. Jongeneel, F. Jotereau, J.C. Cerottini, and P. Romero. 1998. Enhanced generation of specific tumor-reactive CTL in vitro by selected Melan-A/MART-1 immunodominant peptide analogues. *J. Immunol.* 160:1750–1758.

36. Kalergis, A.M., E.C. Goyarts, E. Palmieri, S. Honda, W. Zhang, and S.G. Nathenson. 2000. A simplified procedure for the preparation of MHC/peptide tetramers: chemical biotinylation of an unpaired cysteine engineered at the C-terminus of MHC-I. *J. Immunol. Methods.* 234:61–70.

37. Sallusto, F., D. Lenig, R. Forster, M. Lipp, and A. Lanzavecchia. 1999. Two subsets of memory T lymphocytes with distinct homing potentials and effector functions. *Nature.* 401:708–712.

38. Westermann, J., V. Blaschke, G. Zimmermann, U. Hirschfeld, and R. Pabst. 1992. Random entry of circulating lymphocyte subsets into peripheral lymph nodes and Peyer's patches: no evidence in vivo of a tissue-specific migration of B and T lymphocytes at the level of high endothelial venules. *Eur. J. Immunol.* 22:2219–2223.

39. Kaech, S.M., and R. Ahmed. 2001. Memory CD8+ T cell differentiation: initial antigen encounter triggers a developmental program in naive cells. *Nat. Immunol.* 2:415–422.

40. Loftus, D.J., C. Castelli, T.M. Clay, P. Squarcina, F.M. Marincola, M.I. Nishimura, G. Parmiani, E. Appella, and L. Rivoltini. 1996. Identification of epitope mimics recognized by CTL reactive to the melanoma/melanocyte-derived peptide MART-1(27-35). *J. Exp. Med.* 184:647–657.

41. Loftus, D.J., P. Squarcina, M.B. Nielsen, C. Geisler, C. Castelli, N. Odum, E. Appella, G. Parmiani, and L. Rivoltini. 1998. Peptides derived from self-proteins as partial agonists and antagonists of human CD8+ T-cell clones reactive to melanoma/melanocyte epitope MART1(27-35). *Cancer Res.* 58:2433–2439.

42. Barton, G.M., and A.Y. Rudensky. 1999. Requirement for diverse, low-abundance peptides in positive selection of T cells. *Science.* 283:67–70.

43. Klein, L., and B. Kyewski. 2000. Self-antigen presentation by thymic stromal cells: a subtle division of labor. *Curr. Opin. Immunol.* 12:179–186.

44. Dietrich, P.Y., P.R. Walker, A.L. Quiquerez, G. Perrin, V. Dutoit, D. Liénard, P. Guillaume, J.C. Cerottini, P. Romero, and D. Valmori. 2001. Melanoma patients respond to a cytotoxic T lymphocyte-defined self-peptide with diverse and nonoverlapping T-cell receptor repertoires. *Cancer Res.* 61:2047–2054.

45. Miller, J.F., and W.R. Heath. 1993. Self-ignorance in the peripheral T-cell pool. *Immunol. Rev.* 133:131–150.

46. Ohashi, P.S., S. Oehen, K. Buerki, H. Pircher, C.T. Ohashi, B. Odermatt, B. Malissen, R.M. Zinkernagel, and H. Hengartner. 1991. Ablation of "tolerance" and induction of diabetes by virus infection in viral antigen transgenic mice. *Cell.* 65:305–317.

47. Valmori, D., V. Dutoit, D. Lienard, F. Lejeune, D. Speiser, D. Rimoldi, V. Cerundolo, P.Y. Dietrich, J.C. Cerottini, and P. Romero. 2000. Tetramer-guided analysis of TCR beta-chain usage reveals a large repertoire of melan-A-specific CD8+ T cells in melanoma patients. *J. Immunol.* 165:533–538.

48. Sugita, S., K. Sagawa, M. Mochizuki, S. Shichijo, and K. Itoh. 1996. Melanocyte lysis by cytotoxic T lymphocytes recognizing the MART-1 melanoma antigen in HLA-A2 patients with Vogt-Koyanagi-Harada disease. *Int. Immunol.* 8:799–803.

49. Ogg, G.S., P. Rod Dunbar, P. Romero, J.L. Chen, and V. Cerundolo. 1998. High frequency of skin-homing melanocyte-specific cytotoxic T lymphocytes in autoimmune vitiligo. *J. Exp. Med.* 188:1203–1208.

50. Lang, K.S., C.C. Caroli, A. Muhm, D. Wernet, A. Moris, B. Schittek, E. Knauss-Scherwitz, S. Stevanovic, H.G. Rammensee, and C. Garbe. 2001. HLA-A2 restricted, melanocyte-specific CD8(+) T lymphocytes detected in vitiligo patients are related to disease activity and are predominantly directed against MelanA/MART1. *J. Invest. Dermatol.* 116:891–897.